Internal Equilibrium of the Hammerhead Ribozyme Is Altered by the Length of Certain Covalent Cross-Links

Kenneth F. Blount‡ and Olke C. Uhlenbeck*

Department of Chemistry and Biochemistry, University of Colorado Boulder, UCB 215, Boulder, Colorado 80309

Received January 28, 2002; Revised Manuscript Received March 22, 2002

ABSTRACT: A method was developed that permits covalent cross-links of different linker lengths to be introduced into RNA at defined positions. The previous observation that a cross-link between stems I and II of the hammerhead ribozyme was confirmed and further explored. By examining the catalytic consequences of varying the position and length of this cross-link, we conclude that the previously proposed conformational dampening model cannot sufficiently explain the increase in ligation rate induced by the cross-link. Rather, the cross-link constrains the cleaved hammerhead into a structure that more closely resembles the transition state, thereby increasing the reverse ligation rate relative to a non-cross-linked control.

The hammerhead ribozyme is a small autocatalytic RNA motif that catalyzes site-specific phosphodiester cleavage, producing 5′-OH and 2′,3′-cyclic phosphate products (*1*, *2*). Although the hammerhead can also catalyze the reverse ligation reaction, under most conditions the cleavage-ligation equilibrium (K_{eq}^{int}) favors cleavage by at least 100-fold (*3*). This is somewhat surprising, given that the enthalpy change for forming the strained 2′,3′-cyclic phosphate from a phosphodiester is quite unfavorable (*4*, *5*). The large favorable entropy change upon hammerhead cleavage overcomes the unfavorable enthalpy and has led to the suggestion that an increase in hammerhead dynamics helps to drive the equilibrium in the direction of cleavage (*3*). However, subsequent experiments have revealed that weaker binding of a divalent metal ion to the cleaved hammerhead also contributes significantly to the equilibrium.

In an attempt to modify the dynamics of the hammerhead, a covalent cross-link was introduced between the 2′-positions of residue 2.6 in stem I and 11.5 in stem II, distal to the catalytic core (*6*). This cross-link altered the cleavage−ligation equilibrium such that the cleavage and ligation rates were approximately equal. This dramatic change in the cleavage−ligation equilibrium was entirely due to an increase in the ligation rate, with no effect on the cleavage rate. To account for this observation, it was proposed that the cleaved, non-cross-linked hammerhead undergoes large-scale thermal motions that decrease the efficiency of ligation. By restricting these unfavorable motions, the cross-link could increase the ligation rate.

This model suggests that varying the length of the cross-link might alter the degree of conformational dampening, with a resultant effect on the ligation rate. Specifically, shortening the cross-link potentially could further restrict the motions, thereby increasing ligation, while lengthening the cross-link may reduce ligation. To test this possibility, an alternative procedure was developed to prepare cross-linked hammerheads with different linker lengths, and their catalytic properties were characterized.

EXPERIMENTAL PROCEDURES

General. All TLC was performed on aluminum sheets precoated with a 0.2-mm layer of silica gel 60 F_{254} (Merck, Germany). ^{1}H NMR spectra were recorded on a Bruker AM-400 spectrometer. ^{13}C NMR spectra were recorded on a Varian Inova 500 spectrometer. δ values in ppm relative to tetramethylsilane as an internal standard. Gas chromatograph−mass spectra were taken on Hewlett-Packard 5988A spectrometer. MALDI-TOF1[1] mass spectra were taken on an Applied Biosystems Voyager-DE STR workstation.

Materials. All starting materials for synthesis were reagent grade or higher from Aldrich, except where noted. Solvents were Fisher Scientific ACS grade, except glacial acetic acid (Mallinckrodt). NMR solvents were from Cambridge Isotope Laboratories. 2′-Amino-cytidine phosphoramidite was a generous gift from Wolfgang Pieken (Proligo). 1-Ethyl-3-[3-dimethylaminopropyl]-carbodiimide was from Pierce Biochemicals, and dithiothreitol was from Fisher Biochemicals.

4-Mercapto-butyric Acid. This procedure was adapted from that of Koenig et al. for the synthesis of long-chain mercapto acids (*7*). A total of 5 g of 4-bromobutyric acid (30 mmol), 2.4 g of thiourea (32 mmol), and 125 mL of ethanol were refluxed for 4 h. A solution of 12 g of sodium hydroxide (300 mmol) in 125 mL of ethanol was added, and the solution

* To whom correspondence should be addressed. Olke.Uhlenbeck@colorado.edu

‡ Current address: Department of Chemistry and Biochemistry 0358, University of California, San Diego, La Jolla, CA 92093-0358.

[1] Abbreviations: MALDI-TOF, matrix asssisted laser desorbtion ionization-time-of-flight mass spectrometry; bis-Tris, bis(2-hydroxyethyl)-amino-tris(hydroxy-methyl)-methane; EDTA, ethylenediaminetetraacetic acid; MES, 4-morpholineethanesulfonic acid; EDC, 1-ethyl-3-[3-dimethylaminopropyl]-carbodiimide; PAGE, polyacrylamide gel electrophoresis; DTT, dithiothreitol; HEPES, 4-(2-hydroxyethyl)-1-piperazineethanesulfonic acid; PIPES, 1,4-piperazinebis(ethanesulfonic acid); R^S, cross-linked ribozyme-substrate complex; R^P1, cross-linked ribozyme-product complex.

10.1021/bi025596c CCC: $22.00
Published on Web 04/30/2002

was refluxed 16 h. The white precipitate was isolated by vacuum filtration (Whatman no.1). The filtrate was washed with 100 mL of ice cold absolute ethanol. After resuspending the filtrate in 100 mL of water, 4 N HCl was added dropwise at a rate such that the temperature did not exceed 50 °C until the solution cleared at approximately pH 5. This solution was extracted twice with an equal volume of diethyl ether. After drying of the sample over magnesium sulfate (Fisher Scientific), the organic layer was evaporated at 40 °C. The resultant oil (1.61 g, 13.4 mmol, 45% yield) was used directly in subsequent steps. Analysis: TLC (silica gel; 3 × 10 cm; 79:20:1 HOAc/MeOH/$CHCl_3$) R_f = 0.6, visualized by I_2 stain. δ_H [400 MHz; $CDCl_3$]: 1.75 (2H, m, CH_2), 2.32 (2H, t, CH_2), 2.48 (2H, m, CH_2). δ_C [500 MHz; DMSO-d_6]: 23.3, 28.8, 32.2, 174.1. GC-MS(EI) m/z = 120 [M^+], calculated = 120.02.

N-(Thiophenyl)-phthalimide. This synthesis was performed as described (*8*). A total of 10 g (46 mmol) of phenyldisulfide (Fluka) was suspended in 200 mL of pentane in three-necked flask with gas inlet and outlet. The suspension was cooled and stirred on ice while Cl_2 was bubbled through the mixture until a clear orange solution was obtained (45 min). This solution was added dropwise to a stirred solution of 13.2 g (92 mmol) of phthalimide and 9.3 g (92 mmol) of triethylamine in 100 mL of *N*,*N*-dimethylformamide. After stirring an additional 45 min, this solution was poured into 50 mL of ice water. The pentane was allowed to evaporate overnight, and the resulting precipitate was filtered, washed with 100 mL of cold water and 50 mL diethyl ether, and dried in a vacuum desiccator overnight. The crude product was recrystallized from absolute ethanol (11.9 g, 46.5 mmol, 51.6% yield). Analysis: δ_H [400 MHz; $CDCl_3$]: 7.32 (3h, m, aromatic), 7.60 (2h, m, aromatic), 7.79 (2h, m, aromatic), 7.93 (2h, m, aromatic). δ_C [500 MHz; $CDCl_3$]: 124.0, 129.3, 130.9, 132.0, 134.7, 135.0, 167.7.

2-(Phenyldithio)-acetic Acid. This procedure was adapted from that of Ramaswami (*8*). Rather than recrystallization, the final product was purified by flash chromatography. A total of 1 g (3.9 mmol) of *N*-(thiophenyl)-phthalimide and 0.42 g (4.6 mmol) of mercaptoacetic acid were suspended in 75 mL of argon-purged benzene. This mixture was refluxed, with a drying tube, 72 h, at which point a deep yellow color developed. After cooling of the sample on ice, the solution was vacuum filtered (Whatman no. 1), and the eluent was evaporated. The resulting residue was suspended in 40 mL of methylene chloride and loaded onto 75 g of alumina (80−200 mesh, Fisher Scientific) that had been preequilibrated with methylene chloride. After washing of the sample with 250 mL of methylene chloride and 250 mL of methylene chloride/methanol (20:1), the product was eluted in 200 mL of methylene chloride/methanol/acetic acid (95:5:1). The eluent was evaporated to approximately 10 mL, at which point 50 mL of hexanes was added. This procedure was repeated twice more to remove residual acetic acid. A final evaporation step yielded a pale yellow solid (0.305 g, 1.5 mmol, 33% yield). Analysis: TLC (silica gel; 3 × 10 cm; 94:5:1 $CHCl_3$/MeOH/HOAc) R_f = 0.44, visualized by UV shadow. δ_H [400 MHz; $CDCl_3$]: 3.51 (2H, s, CH_2), 7.27 (1H, t, aromatic-*o*), 7.34 (2H, dd, aromatic-*m*), 7.56 (2H, d, aromatic-*p*). δ_C [500 MHz; $CDCl_3$]: 40.4, 127.8, 129.0, 135.8, 174.9. GC-MS(EI) m/z = 200 [M^+], calculated = 200.0.

3-(Phenyldithio)-propionic Acid. 3-(Phenyldithio)-propionic acid was synthesized and purified in the same manner as 2-(phenyldithio)-acetic acid. Starting materials were 1 g (3.9 mmol) of *N*-(thiophenyl)-phthalimide and 0.42 g (4.0 mmol) of 3-mercaptopropionic acid in 75 mL of argon-purged toluene. The final isolated product was a white solid (0.205 g, 0.96 mmol, 24% yield). Analysis: TLC (silica gel; 3 × 10 cm; 94:5:1 $CHCl_3$/MeOH/HOAc) R_f = 0.38, visualized by UV shadow. δ_H [400 MHz; $CDCl_3$]: 2.79 (2H, t, CH_2−S), 2.95 (2H, t, CH_2−C═O), 7.24 (1H, t, aromatic-*p*), 7.33 (2H, t, aromatic-*o*), 7.54 (2H, d, aromatic-*m*). δ_C [500 MHz; $CDCl_3$]: 32.9, 33.8, 127.3, 128.0, 129.3, 137.0. GC-MS(EI) m/z = 214 [M^+], calculated = 214.0.

4-(Phenyldithio)-butyric Acid. 4-(Phenyldithio)-butyric acid was synthesized and purified in the same manner as 2-(phenyldithio)-acetic acid. Starting materials were 1 g (3.9 mmol) of *N*-(thiophenyl)-phthalimide and 0.42 g (4.0 mmol) of 3-mercaptopropionic acid in 75 mL of argon-purged toluene. The product was eluted in 200 mL of methylene chloride/methanol/acetic acid 88:10:2. The final isolated product was a white solid (0.205 g, 0.96 mmol, 24% yield). Analysis: TLC (silica gel; 3 × 10 cm; 94:5:1 $CHCl_3$:MeOH:HOAc) R_f = 0.38, visualized by UV shadow. δ_H [400 MHz; $CDCl_3$]: 2.0 (2H, q, −C−CH_2−C), 2.47 (2H, t, CH_2−S), 2.78 (2H, t, CH_2−S), 7.25 (1H, m, aromatic-*p*), 7.33 (2H, t, aromatic-*o*), 7.53 (2H, d, aromatic-*m*). δ_C [500 MHz; $CDCl_3$]: 23.4, 32.1, 37.5, 127.0, 127.8, 129.0, 137.1. GC-MS(EI) m/z = 228 [M^+], calculated = 228.0.

RNA Synthesis and Purification. The 2′-amino cytosine-containing oligonucleotides were synthesized on an ABI synthesizer using standard phosphoramidite chemistry and deprotected as previously described (*9*). Each oligonucleotide was purified by fractionation on 20% denaturing PAGE. After elution overnight from the gel in a buffer containing 50 mM bis-Tris pH 6.5, 1 M NaCl, and 10 mM EDTA, oligonucleotides were ethanol precipitated and resuspended in water. The mass of each was confirmed using MALDI-TOF mass spectrometry, using 2′-hydroxy-picolinic acid matrix. All spectra showed only one peak of appropriate mass.

Amidation of 2′-Amines. For amidation, 6 nmol of each 2′-amino-cytosine containing RNA was incubated for 1 h at 37 °C in 200 μL of a solution containing 100 mM MES pH 6.5, 20 mM cross-linking reagent, and a 1:10 dilution of a freshly prepared aqueous solution of 150mM EDC. After the RNA was ethanol precipitated and resuspended, the amidation reaction was repeated, followed by ethanol precipitating and resuspending in a volume to give an approximate concentration of 50 μM RNA. The amidated ribozyme strand was reduced to the free thiol form by incubation for 1 h at 37 °C in 100 mM Tris pH 8.5 and 20 mM DTT. This solution was desalted on a Pharmacia Microbiospin G-25 spin column to remove DTT. The concentration of the amidated (and reduced where appropriate) products were determined by UV absorbance, and the identity of each was verified by MALDI-TOF MS, using 2-hyroxy-piccolinic acid matrix. All spectra showed only one peak, corresponding to the correct product.

Preparation of Cross-Linked Hammerheads. For preparation of the R^S complex, 250 pmol of the substrate strand, conjugated with the cross-linker, was 5′-labeled with approximately 1.2 mCi 5′-[γ^{32}P]-ATP for 1 h at 37 °C, ethanol

precipitated, and resuspended in 41 μL of water. This was combined with 400 pmol of the conjugated, reduced ribozyme strand to a total volume of 80 μL. This solution, containing 200 mM HEPES pH 7.5 and 1 mM EDTA, was heated to 95 °C for 5 min to disrupt aggregates and incubated at 37 °C for 1.5 h. To 40 μL of this solution, $MgCl_2$ was added to a final concentration of 15 mM. This was incubated 30 additional minutes at 37 °C to prepare the R^P1 complex. Both R^S and R^P1 were then purified on a 20% denaturing polyacrylamide gel, and eluted as above, except that elution was for only 4 h. After ethanol precipitating, both R^S and R^P1 were resuspended in 50 μL of water.

Internal Equilibrium Measurements (K_{eq}^{int}). The cleavage-ligation equilibrium was measured by combining purified R^P1 with 5.3 μM 3′-product (P2α10) in 107 mM HEPES pH 7.5. After heating this solution at 95 °C for 5 min and slow-cooling to 25 °C over 1.5 h, $MgCl_2$ was added to a final concentration of 10 mM. This solution was divided into seven aliquots, each of which was layered with 10 μL of mineral oil and incubated at temperatures ranging from 5 to 35 °C. Three time points were taken from each aliquot between 18 and 24 h and quenched as described above. R^S and R^P1 were fractionated and quantitated, and the equilibrium in the reverse direction ([S]/[P]) was determined at each temperature. The data were fit to a standard van't Hoff equation:

$$[R^S]/[R^P1] = \exp[-(\Delta H/RT) + (\Delta S/R)]$$

The enthalpic and entropic components of the forward equilibrium are the inverse sign of these values.

Cleavage Rate Measurement (k_{obs}). The single-turnover rate of cleavage was measured as previously described (*6*). R^S was incubated in 107 mM HEPES pH 7.5, 1 mM EDTA at 95 °C for 5 min, followed by a slow-cooling to 25 °C over 1.5 h. Cleavage was initiated by adding $MgCl_2$ to a final concentration of 10.93 mM. Time points for the reaction were quenched by diluting into 5 vol of a solution of 50 mM EDTA in 80% formamide on ice and fractionated on 20% denaturing PAGE. Bands were quantitated using a Molecular Dynamics Storm phosphorimager. The fraction cleaved was plotted as a function of time and fit to the following equation:

$$(R^P1/(R^P1 + R^S))_t = (R^P1/(R^P1 + R^S))_0 + (R^P1/(R^P1 + R^S))_\infty[1 - \exp(-k_{obs}t)]$$

Rate of Approach to Equilibrium (k_{rev}). The rate of approach to equilibrium from the reverse direction was measured by combining purified R^P1 with 5.3 μM 3′-product (P2α10) in 107 mM PIPES pH 7.5, 1 mM EDTA. After this solution was heated at 95 °C 5 min and slow-cooled to 25 °C over 1.5 h, $MgCl_2$ was added to a final concentration of 10.93 mM to initiate ligation. Time points for the reaction were quenched by diluting into 5 vol of a solution of 50 mM EDTA in 80% formamide on ice and fractionated on 20% denaturing PAGE. Bands were quantitated using a Molecular Dynamics Storm phosphorimager. The fraction ligated was plotted as a function of time and fit to the following equation:

$$(R^S/(R^P1 + R^S))_t = (R^S/(R^P1 + R^S))_0 + (R^S/(R^P1 + R^S))_\infty[1 - \exp(-k_{rev}t)]$$

RESULTS

Preparing Hammerheads with Varying Cross-Linker Lengths. The hammerhead ribozyme used in this study is hammerhead α10 (HHα10; Figure 1a), the same used previously for cross-linking studies (*6*). This hammerhead is formed by joining a 21-nucleotide ribozyme strand and a 31-nucleotide substrate strand via stems I and II. The 7 base-pair stem I results in the 3′-product, P2, remaining stably bound after cleavage, thereby facilitating measurement of the ligation reaction. The structure of HHα10 shown in Figure 1b was modeled by adding two A-form base pairs onto both stem I and stem II of the crystal structure of an all-RNA hammerhead (*10*). The originally characterized cross-link had an extended length of 11.75 Å, which should easily span the 5 Å distance between the 2′-positions of residues 11.5 and 2.6 in this structure. The initial goal was to prepare longer and shorter cross-links at the same site.

Two methods have been reported for covalently cross-linking two specifically placed 2′-amine groups within RNA. One approach involved conjugation of either an aryl isothiocyanate or alkyl isocyanate (2-isocyanatoethyl 2-pyridyl disulfide) cross-linking reagent to the two 2′-amines (*11*). After conjugation, the 2-pyridyl disulfide-containing cross-linking reagents were reduced to their free thiol forms, and subsequent oxidation formed the disulfide cross-link. The end result of this method was a reversible disulfide cross-link conjugated to the 2′-positions via a ureido linkage. A similar method involved conjugation of a 2-pyridyl disulfide-containing alkyl succinimidyl ester cross-linking reagent (*N*-succinimidyl 3-[2-pyridyldithio]propionate) to the 2′-amines (*12*). A subsequent disulfide exchange reaction yielded the reducible cross-linker, conjugated to the riboses via 2′-amido linkages. These two methods essentially differ only in the 2′-linkage. Both form a reducible alkyl or aryl cross-link of a specific length. To simplify the synthesis of different linker lengths, we have developed an alternative method for forming a reducible covalent cross-link between 2′-positions.

This new method uses *n*-(phenyldithio)-alkanoic acid as the basic cross-linking reagent (**4**), which can be readily synthesized in different lengths (Scheme 1). An *n*-bromo-alkanoic acid of one, two, or three carbons (**1**) is treated with thiourea yielding the *n*-thioureido-alkanoic acid, which is subsequently hydrolyzed and protonated to yield the *n*-mercapto-alkanoic acid (**2**). *N*-Thiophenyl-phthalimide (**3**) (prepared by chlorination of phenyl disulfide and reaction with phthalimide) is reacted with **2** to yield the *n*-(phenyldithio)-carboxylic acid cross-linking reagents (**4a**, **4b**, and **4c**). The acetamido, propionamido, and butyramido (4-, 6-, and 8-carbon) forms of this reagent have been synthesized, purified, and characterized by proton and carbon NMR and mass spectrometry.

The preparation of HHα10 with a 6-carbon cross-link between residues 11.5 and 2.6 is summarized in Figure 2. A single 2′-amino-cytidine was incorporated through chemical synthesis in both the substrate and ribozyme strands at residues 11.5 and 2.6, respectively. The carboxylic acid moiety of 3-(phenyldithio)-propionic acid (**4b**) was coupled

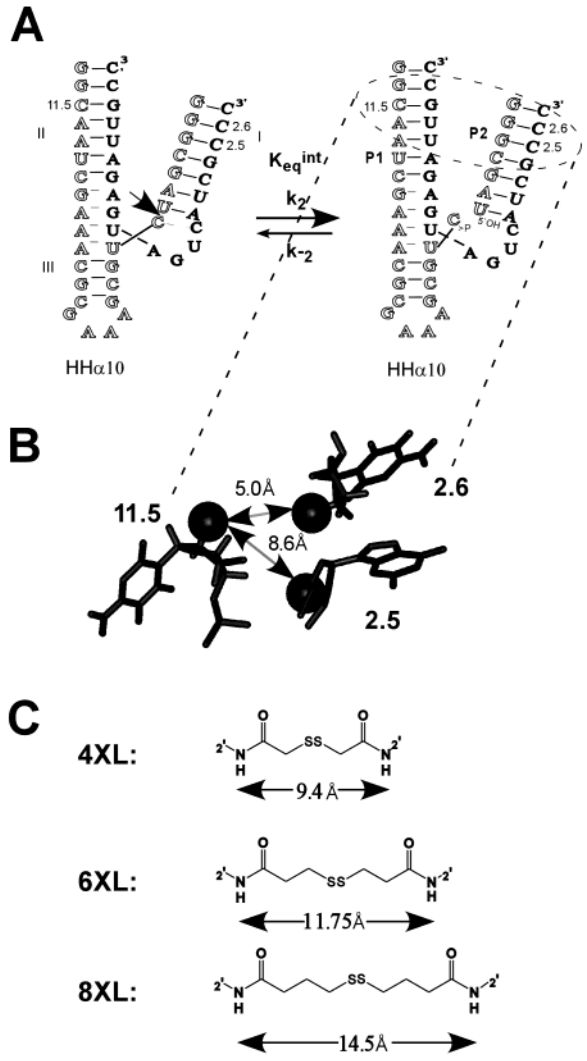

FIGURE 1: Design of cross-linked hammerheads. (A) HHα10 with the substrate strand shown in outlined letters and the ribozyme strand in filled letters. Residues involved in cross-linking—11.5, 2.6, and 2.5—are numbered. The 3′-product, P2, is terminated at the cleavage site in a 5′-hydroxyl, while the 3′-product, P1, is terminated at the cleavage site in a 2′,3′-cyclic phosphate. (B) The structure was constructed by modeling two A-form base-pairs onto the ends of stems I and II of the crystal structure of an all-RNA hammerhead ribozyme (*10*). (C) The chemical structures of the 4-, 6-, and 8-carbon cross-links. The distance shown is the estimated extended 2-prime to 2-prime length of each cross-link.

to the 2′-amine in each strand using the water-soluble carbodiimide 1-ethyl-3-(3-dimethylaminopropyl)-carbodiimide (EDC). The higher nucleophilicity of the 2′-amine permits selective conjugation to the exclusion of base amines (*13*). The specificity and yield of the conjugation reaction were confirmed by observing the formation of a product of higher mass with MALDI-TOF mass spectroscopy. Generally, the efficiency of the conjugation reaction was >95%, while the mass of an all 2′-OH oligonucleotide did not change upon reaction. Because the yields were high, the 2′-conjugated oligonucleotides were used directly, without additional purification. After reducing the ribozyme strand to the mercapto form with dithiothreitol, the two strands were annealed, and the disulfide exchange reaction formed the cross-linked ribozyme−substrate complex, R^S. The cross-linked ribozyme-5′-product complex, R^P1, was prepared by adding 15 mM $MgCl_2$ to R^S and incubating at 37 °C for 45 min. Both the R^S and R^P1 complexes were purified on a 20% denaturing polyacrylamide gel. Although the yields of the disulfide exchange reaction were low, sufficient material was purified to characterize the cleavage or ligation of both complexes.

Cleavage Properties of a Hammerhead with a 6-Carbon Cross-Link between 11.5 and 2.6. Because the six-carbon linker prepared with this method is chemically identical to the previously described hammerhead cross-link made by a different method, its cleavage properties should be identical (*6*). To test whether the cleavage−ligation equilibrium (K_{eq}^{int}) was indeed shifted, the purified R^P1 complex was equilibrated with an excess of the 3′-product P2 at several different temperatures at pH 7.5 in the presence of 10 mM $MgCl_2$ for 24 h. Aliquots of the reaction were quenched at three time points between 18 and 24 h by 5-fold dilution into 80% formamide containing 50 mM EDTA. Following fractionation on a denaturing polyacrylamide gel, the ratio of R^S to R^P1 at each temperature was quantitated (Figure 3). As previously observed, the 6-carbon link between 11.5 and 2.6 dramatically increases the amount of ligated product at each temperature. For example, at 25 °C, K_{eq}^{int} for the cross-linked hammerhead is 4.35, compared to 95.5 for the non-cross-linked control. At temperatures below 20 °C, the equilibrium deviates from van't Hoff behavior. Experiments that measure the reaction from the forward direction do not deviate as much from van't Hoff behavior and confirm the same K_{eq}^{int} values measured from the reverse direction at temperatures above 20 °C (Blount and Uhlenbeck, unpublished data). Therefore, it is likely that the deviation in the reverse direction is the result of the formation of an inactive form of the R^P1 complex at lower temperatures. For this reason, the data below 20 °C were not used to determine ΔS and ΔH for the internal equilibrium. The thermodynamic parameters determined for the hammerhead with the 6-carbon cross-link are shown in Table 1. As previously reported, the cross-link increases the overall free energy of the equilibrium (in the forward direction) by nearly 2 kcal mol^{-1} compared to the non-cross-linked control.

To confirm this shift in equilibrium, the rates of cleavage and ligation were also measured. The observed rate of cleavage (k_{for}) was measured by monitoring the conversion R^S to R^P1 at pH 7.5 in the presence of 10 mM $MgCl_2$. Because the calculated dissociation rate for the 3′-product, P2, is of the same order as the cleavage rate, k_{for} may reflect a small component of the reverse reaction. Nevertheless, the observed cleavage rate for the cross-linked hammerhead (0.45 ± 0.06 min^{-1}) compares favorably with the value measured previously and with the non-cross-linked control (1.17 ± 0.08 min^{-1}). Conversely, the rate of ligation was measured by combining R^P1 with a ~1000-fold excess of P2 and monitoring the formation of R^S in the presence of 10 mM $MgCl_2$. The rate of formation of R^S, k_{rev}, reflects the sum of the cleavage and ligation rates ($k_{rev} = k_2 + k_{-2}$) and was too fast to accurately measure at pH 7.5. Therefore, the ligation rate measurements were performed at pH 6.5. Because the cleavage and ligation rates vary equally and linearly with pH (*3*), the internal equilibrium is the same at both pH values, and k_{-2} can be accurately calculated at pH 6.5. The ligation rate thus measured (0.12 min^{-1}) agrees well with the previously reported value (0.1 min^{-1}) and is nearly

Scheme 1

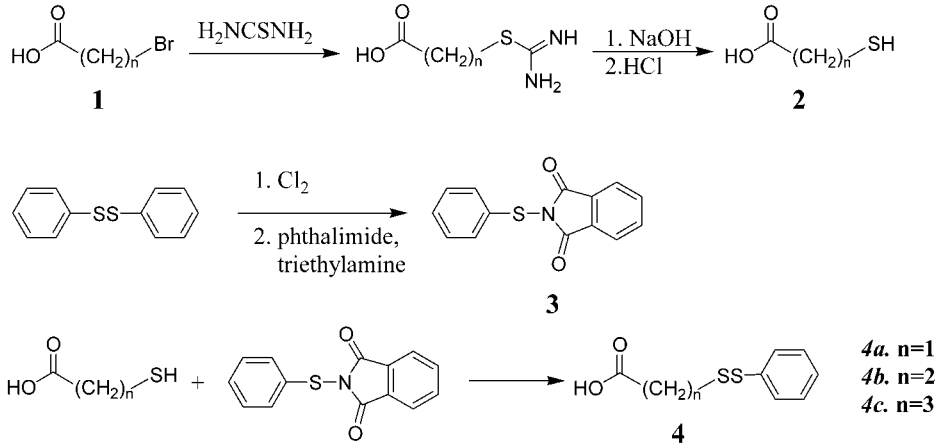

40-fold faster than the non-cross-linked control (*14*). Despite the modest error typically observed in measuring hammerhead cleavage or ligation rates, the $K^{int}_{eq(298K)} = 3.8$ calculated at pH 6.5 from these rates agrees quite well with the $K^{int}_{eq(298K)} = 4.4$ determined directly at pH 7.5.

To confirm that the increase in ligation is in fact due to the cross-link, K^{int}_{eq} was measured after breaking the cross-link. Purified, refolded R^P1 was incubated with a 1000-fold excess of P2 for 30 min at 37 °C in the presence of 15 mM DTT. Upon addition of 10 mM $MgCl_2$, the internal equilibrium was measured at 5, 15, and 25 °C as described above. At each temperature, the amount of ligated substrate formed was the same as for the non-cross-linked control, and $K^{int}_{eq298K} = 85.40$. Thus, the increase in the ligation rate is dependent upon the cross-link being intact.

To confirm that the observed cleavage of the cross-linked hammerhead represented genuine hammerhead catalysis, we measured the rate of cleavage as a function of divalent and monovalent ions. Hammerhead cleavage is characterized by a very specific divalent and monovalent metal ion dependence (*15*−*17*). Between 3 and 15 mM $MgCl_2$ and between 2 and 4 M $LiCl_2$, the hammerhead cross-linked between 11.5 and 2.6 cleaves with the same magnesium or lithium concentration dependence as the non-cross-linked control (data not shown). It can, therefore, be concluded that the cross-link does not change the mode of catalysis.

Varying the Cross-Linker Length between 11.5 and 2.6. To investigate the effect of linker length, hammerheads with 4- or 8-carbon linkers between 11.5 and 2.6 were also characterized. When fully extended, the 4- and 8-carbon cross-linkers can span a distance of 9.5 and 14.5 Å, respectively, between 2′-positions (Figure 1c). The temperature dependence of K^{int}_{eq} revealed that linker length has no detectable effect on K^{int}_{eq} at every temperature tested (Figure 3; Table 1). Indeed, the free energy determined from these data vary by less than 0.1 kcal mol^{-1} among the three linker lengths. Similarly, the enthalpic and entropic component vary only slightly among the three linker lengths. To further confirm these equilibrium data, the rates of cleavage and ligation were measured for both the longer and shorter cross-link as described above. The observed cleavage rates for the 4- and 8-carbon linked hammerheads (0.45 ± 0.06 and 0.30 ± 0.02, respectively) were identical to the 6-carbon version. Likewise, the ligation rates were unchanged among the different linker lengths. Thus, contrary to expectation, altering the linker length between residues 11.5 and 2.6 has no effect on the cleavage−ligation equilibrium of the hammerhead.

Cross-Linking Residues 11.5 and 2.5. For all three hammerheads with the 11.5−2.6 cross-link, the linker lengths exceeds the 2-prime to 2-prime distance between these residues in the structure, suggesting the cross-link could act as a loose tether (Figure 1c). It would be useful to have data for a cross-link whose length approaches the actual distance in the structure. Because the cross-linking reagents described here cannot be synthesized in shorter versions, this was not possible at these two residues. However, if residue 2.5 is used instead of 2.6, the distance to the 2-prime position of residue 11.5 is approximately 8.6 Å (Figure 1c). This approaches the extended length of the 4-carbon cross-link—9.4 Å. Therefore, cross-linked hammerheads with each of the three linker lengths between 11.5 and 2.5 were prepared, and their cleavage properties were characterized.

The internal equilibrium of a hammerhead with an 8-carbon cross-link between 11.5 and 2.5 is also shifted relative to the non-cross-linked hammerhead, to favor cleavage and ligation approximately equally (Table 2). Thermodynamically, relative to a non-cross-linked hammerhead an 8-carbon cross-link between residues 11.5 and 2.5 increases $\Delta G°$ for the equilibrium by approximately 2 kcal mol^{-1}. This $\Delta G° = -1.05$ kcal mol^{-1} is very similar to the average $\Delta G° = -0.86$ for the three linker lengths between 11.5 and 2.6. Interestingly, the enthalpic and entropic components of the free energy are slightly different for this cross-linked hammerhead. The enthalpic component is approximately 8 kcal mol^{-1} less favorable than the 11.5 to 2.6 cross-linked hammerhead, while the entropic component is nearly 30 eu more favorable.

Surprisingly, as the linker length between 11.5 and 2.5 is reduced, the internal equilibrium for the cross-linked hammerhead approaches that of the non-cross-linked control. Decreasing the linker length from 14.5 to 11.75 Å (6 carbons) increased K^{int}_{eq} by 2-fold with a corresponding 0.4 kcal mol^{-1} decrease in free energy. Strikingly, as the linker length between 11.5 and 2.5 is further reduced to 9.5 Å (four carbons), the internal equilibrium is increased an additional 6-fold to within 2-fold of K^{int}_{eq} for the non-cross-linked control—nearly 10-fold larger than the 8-carbon linker. This corresponds to more than a 1 kcal mol^{-1} decrease in the free

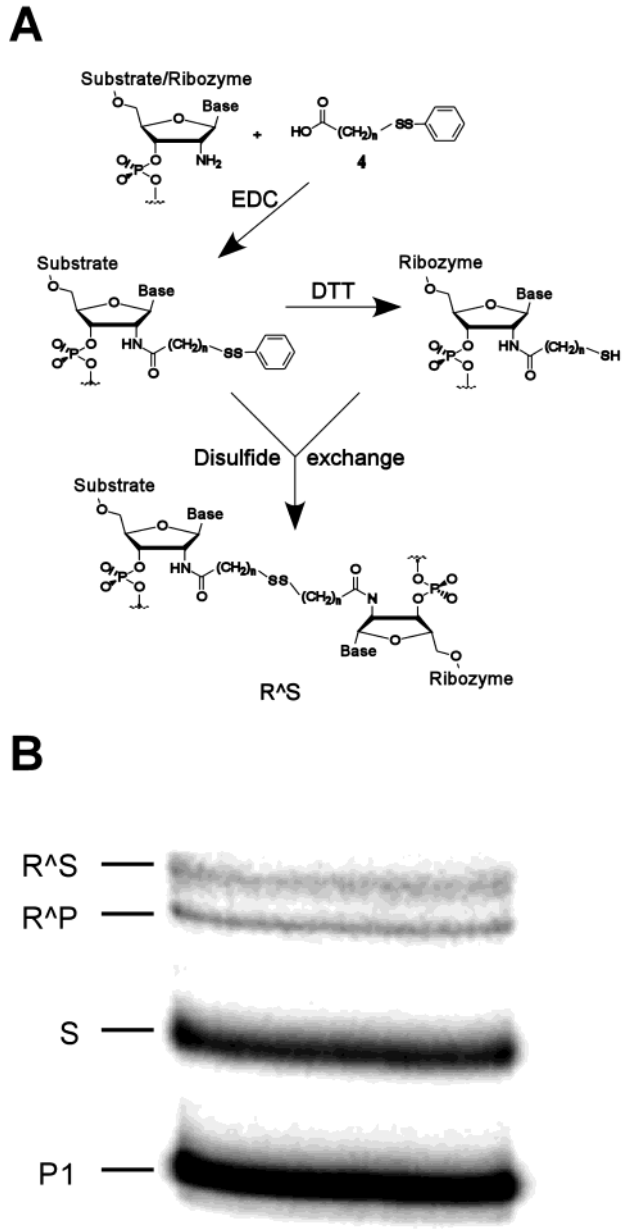

FIGURE 2: Preparation and purification of cross-linked hammerhead ribozymes. (A) Using EDC, the cross-linking reagent (4a, 4b, or 4c) is coupled to a single specifically placed 2′-amine in each strand of the hammerhead. The disulfide is reduced to a free thiol in the ribozyme strand (gray). After the ribozyme and substrate strands are annealed, disulfide exchange forms the cross-linked R^S complex, which is subsequently cleaved in magnesium to yield R^P1. (B) Purification of cross-linked R^S and R^P1 complexes on 20% denaturing PAGE.

energy of the equilibrium. Equally striking is the difference among the enthalpic and entropic components. The enthalpy for the 4-carbon linker is nearly 10 kcal mol^{-1} more favorable than the 8-carbon linker. Likewise, the entropy decreases by nearly 30 eu. Thus, contrary to expectations, decreasing the linker length between 11.5 and 2.5 increased the internal equilibrium to favor cleavage nearly as well as the non-cross-linked control.

DISCUSSION

Using a new method for forming covalent cross-links in RNA, we confirmed the previous observation that an 11.75 Å cross-link between the 2′-positions of residues 11.5 and 2.6 in the hammerhead results in a 25-fold increase in the rate of the reverse ligation reaction without affecting the cleavage rate. As previously observed, the cleavage rate of the hammerhead is unaffected by the introduction of the cross-link, suggesting that the rate-determining step of the reaction is not altered. A conformational dampening model was previously proposed to explain the dramatic change in hammerhead ligation. In this model, it was assumed that a large increase in thermal motions after cleavage helps to drive

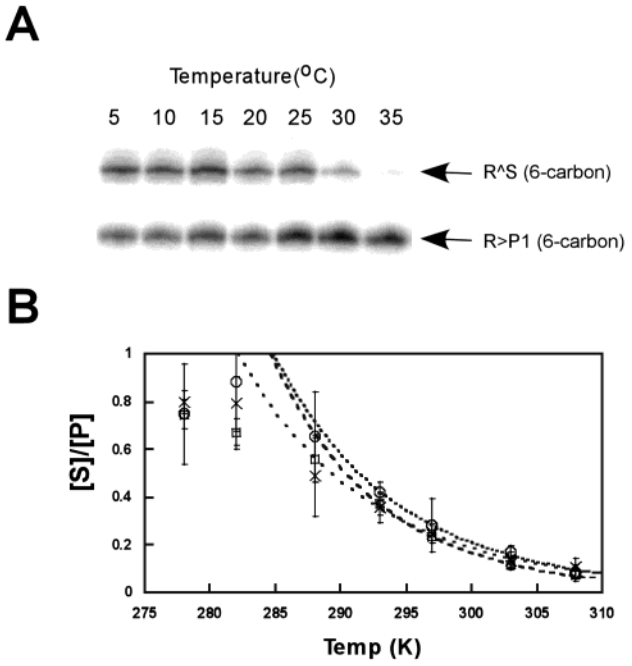

FIGURE 3: Measuring the internal equilibririum (K_{eq}^{int}) for cross-linked hammerheads. (A) 20% denaturing PAGE fractionating R^S complex from R^P1 complex. Temperature range is from 5 to 37 °C. (B) Plot of $1/K_{eq}^{int}$ versus temperature for the hammerhead with a 4-carbon ("X"), 6-carbon (open squares), and 8-carbon (open circles) cross-link between the 2′-positions of residues 11.5 and 2.6. Data are fit to a standard Van't Hoff equation. Since the values thus obtained correspond to the equilibrium in the reverse direction ($1/K_{eq}^{int}$), the entropic and enthalpic components of the free energy of the equilibrium in the forward direction are simply the inverse sign of these.

Table 1: Thermodynamic Parameters for the Non-Cross-Linked Hammerhead and the Hammerheads Cross-Linked between Residues 11.5 and 2.6

	non-XL	4-carbon	6-carbon	8-carbon
$K_{eq\,298K}^{int}$ ([P]/[S])	95.5	4.12 ± 0.65	4.35 ± 0.4	3.89 ± 1.32
ΔH (kcal mol^{-1})	16.9 ± 0.6	15.7 ± 0.97	19.8 ± 0.35	17.5 ± 1.1
ΔS (eu)	65.8 ± 2	55.7 ± 3.3	69.4 ± 1.2	61.4 ± 3.9
ΔG_{298} (kcal mol^{-1})[a]	−2.7	−0.90	−0.88	−0.80

[a] Calculated from $\Delta G = \Delta H - T\Delta S$.

Table 2: Thermodynamic Parameters for the Hammerhead Cross-Linked between Residues 11.5 and 2.5

	4-carbon	6-carbon	8-carbon
$K_{eq\,298K}^{int}$ ([P]/[S])	61.9 ± 37.5	11.1 ± 2.1	6.92 ± 2.5
ΔH (kcal mol^{-1})	18.4 ± 3.6	29.5 ± 1.6	26.9 ± 1.4
ΔS (eu)	69.0 ± 12.6	103.8 ± 5.7	93.8 ± 4.8
ΔG_{298} (kcal mol^{-1})[a]	−2.13	−1.43	−1.05

[a] Calculated from $\Delta G = \Delta H - T\Delta S$.

the internal equilibrium of the non-cross-linked hammerhead toward cleavage. The cross-link was proposed to simply act as a tether between stems I and II, dampening the thermal motions of the cleaved hammerhead enough to shift the internal equilibrium to favor cleavage and ligation equally. While this model provided an adequate explanation for the data, it was curious that all X-ray and solution data suggested that the equilibrium structure of the cleaved hammerhead was not grossly different from the uncleaved form (*18*, *19*), implying that the dynamic motions would average to a similar structure. In addition, it was unclear why an alternate method of constraining molecular motions via circularized hammerhead substrates did not show a large increase in the ligation rate (*20*).

Experiments presented here show that the cleavage−ligation equilibrium of the hammerhead cross-linked between 11.5 and 2.6 is remarkably unaffected when the 11.75 Å cross-link is either decreased to 9.4 Å or increased to 14.5 Å. Not only are the cleavage and ligation rates unaffected, but also the enthalpic and entropic components of the cleavage−ligation equilibrium are virtually unchanged among the three cross-linked hammerheads. Since the length of the cross-link is expected to influence the modes of motion available to the cleaved hammerhead, these results argue against a conformational dampening model. That is, even though all three linker lengths are longer than the 5 Å distance between the 2′-positions of 11.5 and 2.6 in the structure, varying the linker length from 9.4 to 11.5 Å should still significantly alter the conformational flexibility of the hammerhead, with a resultant effect on the cleavage−ligation equilibrium. Because varying the linker lengths does not affect the cleavage−ligation equilibrium, a conformational dampening model seems insufficient to explain the effect of the cross-link.

An alternate possibility is that the effect of the cross-link on the hammerhead ligation reaction is not due to conformational dampening at all. Instead the cross-link may alter the structure of the cleaved hammerhead (R^P) to a form more closely resembling the transition state than the non-cross-linked hammerhead. Specifically, there could be a conformational equilibrium after cleavage for the non-cross-linked hammerhead:

$$RS \rightleftharpoons RP^* \rightleftharpoons RP$$

For the non-cross-linked hammerhead, RP* is a high-energy state resembling the transition state, and thus the conversion of RP* to RP is fast and favors RP. If the cross-link constrains a structure closely resembling RP*, this equilibrium would shift to favor RP*. The resultant accumulation of RP* would increase the reverse ligation rate without affecting the rate of cleavage.

One way to discern between a dynamic or structural model is to examine the properties of additional cross-linked hammerheads. To that end, three additional cross-linked hammerheads were prepared in which one of the 2′-positions cross-linked was moved by only one residue—from 2.6 to 2.5. Although this change has the effect of increasing the distance between the 2′-positions from 5 to 8.4 Å, all three linker lengths still exceed this distance when fully extended. Each of these three cross-linked hammerheads cleaves at the same rate as the non-cross-linked control, emphasizing that the rate-determining step is not changed by the introduction of a cross-link. However, the cleavage−ligation equilibrium does differ significantly among the three linker lengths. While the hammerhead with the longest linker between 11.5 and 2.5 approximates the effects of all three 11.5 to 2.6 cross-links, decreasing the linker length at this new position causes the internal equilibrium to favor ligation less well. That is, the ligation rate decreases with linker length. In fact, the cleavage−ligation equilibrium of the hammerhead with the shortest linker strikingly resembles the non-cross-linked hammerhead.

These data are hard to reconcile with a conformational dampening model. Since all three linker lengths should span the distance between 2′-positions in the structure, all should be able to dampen the conformational dynamics of the cleaved product, with a resultant effect on ligation. Furthermore, shortening the linker should increase dampening, thereby increasing ligation. Neither of these predictions is true for the cross-link between 11.5 and 2.5. Rather than dampening conformational motions, the cross-links seem to affect the structure of an intermediate ribozyme−products complex, RP*, that is near the transition state. By either stabilizing or destabilizing this structure, the cross-links affect the conversion of RP* to the typically observed ribozyme−products complex, RP, thereby affecting the reverse ligation rate. On the basis of this model, the 8-carbon linker between 11.5 and 2.5 (like all three 11.5−2.6 cross-links) stabilizes RP*, while the 4-carbon linker at this position destabilizes RP*, allowing the conversion to RP.

In an effort to more fully understand the structural effects of the cross-links, we dissected the enthalpic and entropic components of the reaction. All three linker lengths between 11.5 and 2.6 decrease the entropy of cleavage relative to the non-cross-linked, but also increase the enthalpy. In contrast, the longer two linkers between 11.5 and 2.5 actually increase the entropy, again suggesting against a conformational dampening model. Yet, further decreasing the cross-linker by only 2.4 Å dramatically changes the entropic and enthalpic components to near the values for the non-cross-linked hammerhead. Clearly, it is difficult to establish a correlation between linker length and the entropic or enthalpic contributions.

This difficulty of interpreting entropic and enthalpic components of the hammerhead reaction has been encountered before. When first determined, the individual components were seemingly easily interpreted (*3*) as an unfavorable enthalpic component (10 kcal mol^{-1}) that corresponds well with the formation of a strained pentacyclic 2′,3′-cyclic phosphate (*4*, *5*) and an entropic term (45 eu) that reflects a large increase in conformational flexibility upon cleavage. This interpretation was subsequently complicated by the observation that the dissociation of a specific metal ion after catalysis contributes significantly to the free energy of the reaction (*21*). In addition, a circularized substrate that was predicted to decrease the entropic contribution actually increased it (*20*). Thus, like previous reports, we find it difficult to interpret changes in the enthalpy or entropy of hammerhead catalysis. Nevertheless, a structural model more plausibly explains these data than a conformational dampening model, given the lack of a trend in the entropic component.

Given a structural model for the effects of cross-links, what can be surmised about the structural details of RP*? One possibility is that RP* is a more closed structure from which P2 cannot dissociate as well. In this case, by constraining this closed form, the cross-links inhibit the release of P2, thereby stimulating the ligation rate. It also seems likely that the structure of RP* is not grossly perturbed by the cross-link, or else changes in the forward cleavage reaction might also be observed. Rather, RP* converts to RP through modest structural changes, likely involving the relative orientation of the 5′-OH and 2′,3′-cyclic phosphate products. The sensitivity of the equilibrium to small changes in linker lengths is consistent with this.

These experiments provide an important precedent for the subtleties of cross-link-induced changes in RNA catalysis. A decrease in the length of a cross-link by only 2.5 Å has changed the enthalpic and entropic components of the ligase reaction in this example by nearly 10 kcal mol^{-1} and 30 eu, respectively. An intriguing possibility is that a similar result could be observed for cross-links nearer the catalytic core, perhaps enhancing the hammerhead cleavage rate.

REFERENCES

1. Forster, A. C., Jeffries, A. C., Sheldon, C. C., and Symons, R. H. (1987) Structural and ionic requirements for self-cleavage of virusoid RNAs and trans self-cleavage of viroid RNA, *Cold Spring Harbor Symp. Quantum Biol. 52*, 249−259.
2. Uhlenbeck, O. C. (1987) A small catalytic oligoribonucleotide, *Nature 328*, 596−600.
3. Hertel, K. J., and Uhlenbeck, O. C. (1995) The internal equilibrium of the hammerhead ribozyme reaction, *Biochemistry 34*, 1744−1749.
4. Kumamoto, J., Cox, J. R., and Westheimer, F. H. (1956) *J. Am. Chem. Soc. 78*, 4858−4860.
5. Gerlt, J. A., Westheimer, F. H., and Sturtevant, J. M. (1975) The enthalpies of hydrolysis of acyclic, monocyclic, and glycoside cyclic phosphate diesters. *J. Biol. Chem. 250*, 5059−5067.
6. Stage-Zimmermann, T. K., and Uhlenbeck, O. C. (2001) A covalent cross-link converts the hammerhead ribozyme from a ribonuclease to an RNA ligase, *Nat. Struct. Biol. 8*, 863−867.
7. Koenig, N. H., Sasin, G. S., and Swern, D. (1958) Organic sulfur derivatives. V. Preparation and properties of some long-chain mercapto acids and related compounds. *J. Org. Chem.* 1525−1530.
8. Ramaswami, V. (1986) Photolabeling studies of polymer-cell surface interaction. Evaluation of 3-[(4-azidophenyl)dithio]-propionic acid as a polymer-bound photolabel. *J. Polym. Sci.: Polymer Chem. Ed. 24*, 241−253.
9. Usman, N., Ogilvie, K. K., Jiang, M.-Y., and Cedergren, R. J. (1987) Automated chemical synthesis of long oligoribonucleotides using 2′−O-silylated ribonucleoside 3′-*O*-phosphoramidites on a controlled-pore glass support: synthesis of a 43-nucleotide sequence similar to the 3′-half molecule of an *Escherichia coli* formylmethionine tRNA. *J. Am. Chem. Soc. 109*, 7845−7854.
10. Scott, W., Finch, J., and Klug, A. (1995) The crystal structure of an all-RNA hammerhead ribozyme: A proposed mechanism for RNA catalytic cleavage. *Cell 81*, 991−1002.
11. Sigurdsson, S. T., Tuschl, T., and Eckstein, F. (1995) Probing RNA tertiary Structure: Interhelical cross-linking of the hammerhead ribozyme, *RNA 1*, 575−583.
12. Cohen, S. B., and Cech, T. R. (1997) Dynamics of thermal motions within a large catalytic RNA investigated by cross-linking with thiol-disulfide exchange. *J. Am. Chem. Soc. 119*, 6259−6268.
13. Sigurdsson, S. T., and Eckstein, F. (1996) Site specific labeling of sugar residues in oligoribonucleotides: reactions of aliphatic isocyanates with 2′ amino groups. *Nucleic Acids Res. 24*, 3129−3133.
14. Hertel, K. J., Herschlag, D., and Uhlenbeck, O. C. (1994) A kinetic and thermodynamic framework for the hammerhead ribozyme reaction. *Biochemistry 33*, 3374−3385.
15. Dahm, S. C., Derrick, W. B., and Uhlenbeck, O. C. (1993) Evidence for the role of solvated metal hydroxide in the hammerhead cleavage mechanism. *Biochemistry 32*, 13040−13045.
16. O'Rear, J. L., Wang, S., Feig, A. L., Uhlenbeck, O. C., and Herschlag, D. (2001) Comparison of the hammerhead cleavage reactions stimulated by monovalent and divalent cations, *RNA 7*, 537−545.
17. Curtis, E., and Bartel, D. P. (2001) Role of metal ions in the hammerhead RNA cleavage reaction. *RNA*, in press.
18. Murray, J. B., Szoke, H., Szoke, A., and Scott, W. G. (2000) Capture and visualization of catalytic RNA enzyme−product complex using crystal lattice trapping and X-ray holographic reconstruction. *Mol. Cell 5*, 279−287.
19. Simorre, J.-P., Legault, P., Hangar, A. B., Michiels, P., and Pardi, A. (1997) A conformational change in the catalytic core of the hammerhead ribozyme upon cleavage of an RNA substrate. *Biochemistry 36*, 518−515.
20. Stage-Zimmermann, T. K., and Uhlenbeck, O. C. (1998) Circular substrates of the hammerhead ribozyme shift the internal equilibrium further towards cleavage. *Biochemistry 37*, 9386−9393.
21. Long, D. M., LaRiviere, F. J., and Uhlenbeck, O. C. (1995) Divalent metal ions and the internal equilibrium of the hammerhead ribozyme, *Biochemistry 34*, 14435−14440.

BI025596C